Human Molecular Genetics, 2013, Vol. 22, No. 24 ***4914–4928***
doi:10.1093/hmg/ddt341
Advance Access published on July 23, 2013

Highly efficient *in vivo* delivery of PMO into regenerating myotubes and rescue in laminin-α2 chain-null congenital muscular dystrophy mice

Yoshitsugu Aoki[1,2], Tetsuya Nagata[1,*], Toshifumi Yokota[3,4], Akinori Nakamura[5,6], Matthew J.A. Wood[2], Terence Partridge[7,8] and Shin'ichi Takeda[1,*]

[1]Department of Molecular Therapy, National Institute of Neuroscience, National Center of Neurology and Psychiatry (NCNP), Ogawa-Higashi 4-1-1, Kodaira, Tokyo 187-8502, Japan, [2]Department of Physiology, Anatomy and Genetics, University of Oxford, South Parks Road, Oxford OX1 3QX, UK, [3]Department of Medical Genetics, School of Human Development, Faculty of Medicine and Dentistry, University of Alberta, 829 Medical Sciences Building, Edmonton, Canada AB T6G 2H7, [4]The Friends of Garrett Cumming Research & Muscular Dystrophy Canada HM Toupin Neurological Science Endowed Research Chair, 829 Medical Sciences Building, Edmonton, Canada AB T6G 2H7, [5]Department of Medicine (Neurology and Rheumatology), Shinshu University School of Medicine, 3-1-1, Asahi, Matsumoto 390-8621, Japan, [6]Division of Intractable Disease Care Center, Shinshu University Hospital, Matsumoto, 3-1-1, Asahi Matsumoto 390-8621, Japan, [7]Research Center for Genetic Medicine, Children's National Medical Center, 111 Michigan Avenue, NW, Washington, DC 20010, USA and [8]Department of Integrative Systems Biology, George Washington University School of Medicine, 111 Michigan Avenue, NW, Washington, DC 20010, USA

Received April 10, 2013; Revised and Accepted July 12, 2013

Phosphorodiamidate morpholino oligomer (PMO)-mediated exon skipping is among the more promising approaches to the treatment of several neuromuscular disorders including Duchenne muscular dystrophy. The main weakness of this approach arises from the low efficiency and sporadic nature of the delivery of charge-neutral PMO into muscle fibers, the mechanism of which is unknown. In this study, to test our hypothesis that muscle fibers take up PMO more efficiently during myotube formation, we induced synchronous muscle regeneration by injection of cardiotoxin into the tibialis anterior muscle of *Dmd* exon 52-deficient *mdx*52 and wild-type mice. Interestingly, by *in situ* hybridization, we detected PMO mainly in embryonic myosin heavy chain-positive regenerating fibers. In addition, we showed that PMO or 2′-*O*-methyl phosphorothioate is taken up efficiently into C2C12 myotubes when transfected 24–72 h after the induction of differentiation but is poorly taken up into undifferentiated C2C12 myoblasts suggesting efficient uptake of PMO in the early stages of C2C12 myotube formation. Next, we tested the therapeutic potential of PMO for laminin-α2 chain-null *dy^{3K}/dy^{3K}* mice: a model of merosin-deficient congenital muscular dystrophy (MDC1A) with active muscle regeneration. We confirmed the recovery of laminin-α2 chain and slightly prolonged life span following skipping of the mutated exon 4 in *dy^{3K}/dy^{3K}* mice. These findings support the idea that PMO entry into fibers is dependent on a developmental stage in myogenesis rather than on dystrophinless muscle membranes and provide a platform for developing PMO-mediated therapies for a variety of muscular disorders, such as MDC1A, that involve active muscle regeneration.

INTRODUCTION

Duchenne muscular dystrophy (DMD), the most common form of muscular dystrophy, involves progressive deterioration of muscle function. DMD is caused mainly by a frameshift deletion, nonsense or duplication mutations in the *DMD* gene, which encodes the protein dystrophin (1). The milder Becker muscular dystrophy (BMD) typically results from in-frame deletions in the *DMD* gene that allows the expression of limited amounts of an internally truncated but functional protein (2).

*To whom correspondence should be addressed. Tel: +81 423461720; Fax: +81 423461750; Email: takeda@ncnp.go.jp (S.T.); nagatat@ncnp.go.jp (T.N.)

In recent years, RNA-targeted splice-correction therapy by antisense oligonucleotide (AO) in DMD muscle with the object of restoring an in-frame, Becker-like transcript is among the more promising therapeutic approaches to treating DMD (3,4). To this end, systemic administration of AO, such as phosphorodiamidate morpholino oligomers (PMOs), targeting specific exon(s) in the *Dmd* gene has been shown to restore the reading frame and induce body-wide production of partially functional BMD-like dystrophin in mouse and dog models of DMD (5–8). Currently, this method was shown to be promising and safe in phase II trials with PMO (9) or 2′-*O*-methyl phosphorothioate (2′OMePS), which is also the most common AO (10), targeting exon 51 for DMD.

PMO, which has a neutral chemistry, provides outstanding safety characteristics and excellent *in vivo* efficacy and is suitable for human use. Moreover, PMO is being used extensively as a tool for selective inhibition of gene expression in cell culture models. However, the poor delivery of the PMO limits the application of PMO-mediated therapy for DMD or other muscular dystrophies. At present the precise mechanism of PMO entry into dystrophin-deficient muscle fibers is still unknown (11,12). A dominant hypothesis is that PMO enters dystrophin-deficient muscle fibers as a result of abnormal membrane permeability, a so-called 'leaky membrane' (13,14).

Here, we show that embryonic myosin heavy chain (eMHC) and dystrophin double-positive regenerating myotubes can incorporate PMO efficiently into *Dmd* exon 52-deficient *mdx*52 (15) and wild-type (WT) mice. Our *in vitro* studies of C2C12 myoblasts suggest that PMO or 2′OMePS is taken up preferentially into muscle cells during the process of myotube formation. We also tested the therapeutic potential of PMO treatment on the dy^{3K}/dy^{3K} mouse (16): a model of laminin-α2 chain (merosin)-deficient congenital muscular dystrophy (MDC1A) (MIM156225) with active muscle regeneration. Our results support the idea that PMO entry into muscle fibers is dependent on a developmental stage in myogenesis rather than on an intrinsic defect in the membrane of dystrophinless muscle fibers: the 'leaky-membrane' hypothesis. As such it provides a platform for developing PMO-mediated therapies for a variety of muscular disorders, such as MDC1A, that involve active muscle regeneration.

RESULTS

Induction of exon 51 skipping in dystrophin-deficient *mdx*52 but not in WT mice after systemic PMO injection, suggesting abnormally high membrane permeability in *mdx*52 mice

To examine the effect of systemic PMO-mediated exon 51 skipping (Supplementary Material, Fig. S1A), we injected 5-week-old *mdx*52 and BL6 WT mice with a single dose of 51Do (Table 1), which targets the splice donor site of exon 51 of the *Dmd* gene, at a range of doses 80, 160, 320 or 640 mg/kg. Two weeks after the injection, the gastrocnemius muscles were isolated and analyzed by reverse transcription–polymerase chain reaction (RT–PCR). We could detect no skipped bands in WT mice but exon 51 skipping was induced in a highly dose-dependent manner with the range of 80–640 mg/kg doses, showing approximately up to 90% skipping efficiency in *mdx*52 mice by RT–PCR (Supplementary Material, Fig. S1B).

Table 1. AO sequence of PMO or 2′OMePS against exon 51 of the *Dmd* gene of mice used in this study

Name	Position	Sequence
51Do	+10−15	TTGTTTTATCCATACCTTCTGTTTG

Enhancement of dystrophin expression after intramuscular injection of PMO into very actively regenerating TA muscles of *mdx*52 mice at 5 weeks of age

To investigate the mechanism of PMO uptake into muscle fibers, we first evaluated the percentage of centrally nucleated fibers, a marker of regenerated fibers, across a range of ages in *mdx*52 ($n = 3$, each age group). Centrally nucleated fibers appeared around 3 weeks, dramatically increased around 4–5 weeks and reached 80% after 16 weeks in *mdx*52 mice (Fig. 1A and B) (Supplementary Material, Fig. S2). Next, we injected PMO 51Do (400 μg/kg body weight) into both tibialis anterior (TA) muscles of *mdx*52 mice aged 3–32 weeks to induce exon 51 skipping (Fig. 1C) and evaluated the extent of dystrophin expression by immunohistochemistry. Two weeks after the injection, the TA muscles were isolated and analyzed by immunohistochemistry. The percentage of dystrophin-positive fibers was 45% on average when PMO was injected at 4 weeks and approximately 20% when PMO was injected from 6 to 32 weeks (Fig. 1D and E). We found that the percentage of dystrophin-positive fibers was highest when PMO was injected into *mdx*52 mice at age 5 weeks when muscle regeneration was very active.

Classification of dystrophin-positive fibers into two types: Bromodeoxyuridine-positive small-caliber fibers and bromodeoxyuridine-negative normal-caliber fibers in *mdx*52 mice

To further investigate the phase of PMO uptake, we administered bromodeoxyuridine (BrdU) in the drinking water (0.8 mg/ml) for 6 days after a single intramuscular injection of PMO 51Do (400 μg/kg body weight) to label newly regenerated fibers. We injected into TA muscle of *mdx*52 mice aged 5 and 32 weeks. Mice were killed 2 weeks after the PMO injection and TA muscles were removed and analyzed by immunohistochemistry for dystrophin, BrdU and DAPI (Fig. 2A). We found that dystrophin-positive fibers could be classified into two types: BrdU-positive small-caliber fibers with diameters of 30–40 μm and BrdU-negative normal-caliber fibers with diameters of 40–60 μm at 5 and 32 weeks in *mdx*52 mice (Fig. 2B and C). The total numbers of dystrophin-positive fibers were significantly higher in the mice injected with PMO at 5 weeks than at 32 weeks

Table 2. Probe sequences against 51Do for *in situ* hybridization used in this study

Name	Sequence
Positive probe	CAAACAGAAGGTATGGATAAAACAA
Negative probe	TTGTTTTATCCATACCTTCTGTTTG

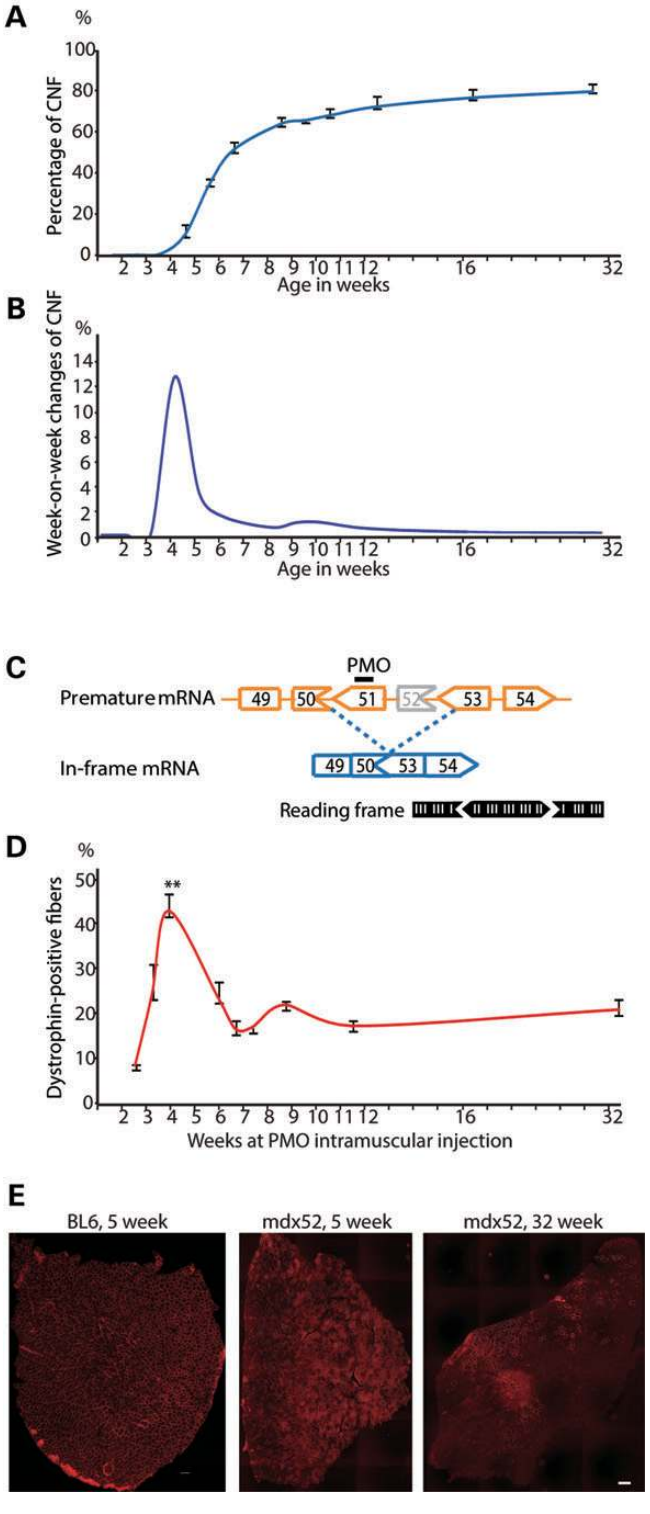

Figure 1. Evaluation of the optimal injection age of PMO into TA muscle in *mdx*52 mice. (A) Percentage of centrally nucleated fibers (CNFs) in TA muscle of *mdx*52 mice according to ages is calculated. The data ($n = 3–5$) are presented as mean ± SD. (B) Week-on-week percentage changes of CNF in TA muscle of *mdx*52 mice according to ages. $n = 3–5$. (C) Strategy for exon 51 skipping in *mdx*52 mouse. Exon 51 skipping by appropriate phosphorodiamidate morpholino oligomers (PMO), indicated by a black line, can restore the reading frame of dystrophin in the *mdx*52 mouse, which lacks exon 52 in the mRNA of the murine *Dmd* gene, leading to out-of-frame products. (D) Percentage of dystrophin-positive fibers according to the injection ages after intramuscular injection of PMO into TA muscle of *mdx*52 mice. The data ($n = 3–4$) are presented as mean ± SD. $^{**}P < 0.01$. (E) Immunohistochemical staining for dystrophin, in the TA muscle of *mdx*52 mice at 5 or 32 weeks of PMO injection age. The restoration of dystrophin in the TA muscles was examined 2 weeks after the injection of PMO (400 μg/kg body weight). One representative out of three independent experiments is shown. BL6: TA muscle from a WT C57/BL6. *mdx*52, 5w: PMO-treated TA muscle from *mdx*52 mice at 5 weeks. *mdx*52, 32w: PMO-treated TA muscle from *mdx*52 mice at 32 weeks. Scale bar: 100 μm.

and the proportion that were of BrdU-positive, small-caliber fibers was also significantly greater (Fig. 2D). Then, we injected PMO (320 mg/kg) into the tail vein of *mdx*52 mice at 5 weeks, which were administered of BrdU in the drinking water (0.8 mg/ml) for 6 days, and performed immunohistochemistry for dystrophin, BrdU and DAPI 2 weeks after the injection (Fig. 2E). A significantly large number of BrdU-positive fibers (303/314, 96.50%) exclusively expressed dystrophin compared with the BrdU-negative fibers (185/943, 19.62%) ($P < 0.001$ by Fisher's exact test) (Fig. 2F). These data suggest that immature regenerated fibers, which are called myotubes, could take up PMO more efficiently than mature fibers.

Efficient PMO entry into regenerated fibers at 4 days after cardiotoxin injection in *mdx*52 mice

In this study, we evaluated the mechanism of PMO entry into small-caliber BrdU-positive fibers. To induce the synchronous regeneration of fibers, cardiotoxin (CTX) was injected intramuscularly into TA muscle of *mdx*52 mice at age 5 weeks (Supplementary Material, Fig. S3). At 1–5 days after CTX injection, PMO (400 μg/kg body weight) targeting the splice donor site of exon 51 was injected into each TA muscle followed by oral administration of BrdU (0.8 mg/ml) for 7 days (Fig. 3A). Two weeks later, TA muscles were obtained and analyzed by RT–PCR, immunohistochemistry and western blotting. The percentage of dystrophin-positive fibers by immunohistochemistry (Fig. 3B and C) and dystrophin expression level by western blotting (Fig. 3D and E) peaked in muscles where PMO had been injected at 4 days after CTX injection. On histology, the TA muscle BrdU and eMHC double-positive small-caliber fibers were seen at high levels at 4 days after CTX injection (Supplementary Material, Fig. S4). These results suggest that PMO was taken up very efficiently when eMHC-positive small-caliber fibers were mainly seen in *mdx*52 mice.

Dramatical induction of exon 51 skipping following systemic PMO injection at 4 days after CTX injection into TA muscles of WT mice

Then we examined the localization of PMO in muscle cryosections using fluorescein-conjugated PMO (f-PMO). First, f-PMO (400 μg/kg body weight) targeting the splice donor site of exon 51 was injected into each TA muscle of *mdx*52 mice at age 5 weeks. Two weeks later, TA muscles were obtained and analyzed by RT–PCR and immunohistochemistry. We found that both PMO and f-PMO could induce similarly efficient exon 51 skipping and dystrophin expression at the fiber membrane (Supplementary Material, Fig. S5A and B).

We next investigated whether the f-PMO is taken up into eMHC-positive regenerated fibers after CTX injection into

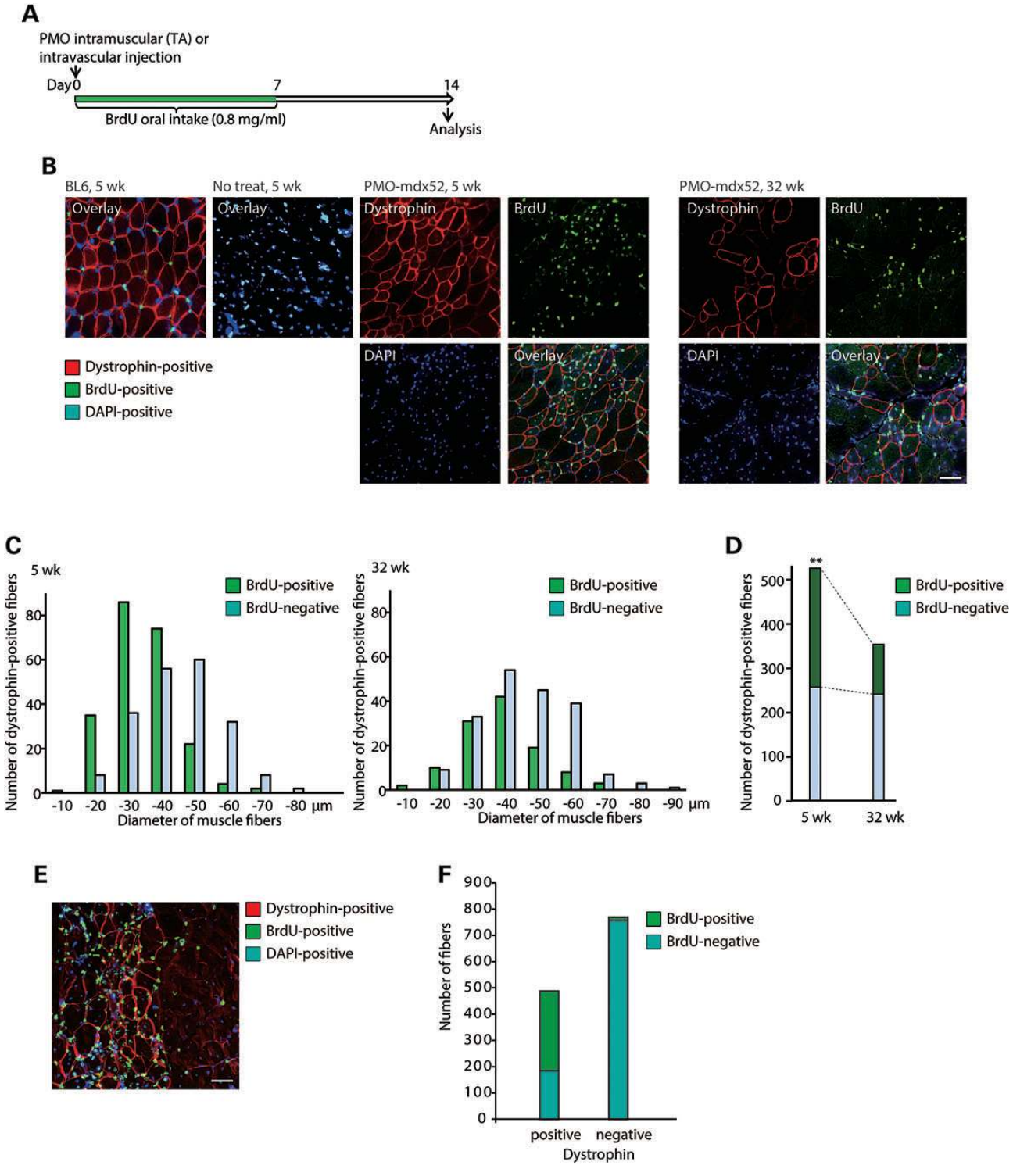

Figure 2. Evaluation of dystrophin-positive fibers using BrdU after intramuscular injection of PMO into the TA muscle of *mdx*52 mice. (A) Experimental model of PMO injection into TA muscle of *mdx*52 mice. PMO (400 μg/kg body weight) was injected into the TA muscles of *mdx*52 mice at 5 or 32 weeks and immunohistochemistry performed 2 weeks after the injection, respectively. (B) Triple immunohistochemical staining of cryosections in TA muscle of *mdx*52 mice at 5 weeks or 32 weeks for dystrophin, BrdU and DAPI. BL6: TA muscle from a WT C57/BL6. No treat: Untreated TA muscle from *mdx*52 mice. Data are representative of four independent experiments. Scale bar, 50 μm. (C) Histogram of BrdU-positive or BrdU-negative fibers among dystrophin-positive fibers in the TA muscle of *mdx*52 mice at 5 or 32 weeks of injection age, $n = 4$. (D) Number of BrdU-positive or BrdU-negative fibers among dystrophin positive fibers at 5 or 32 weeks of injection age in *mdx*52 mice. The data ($n = 4$) are presented as mean ± SD, $^{**}P < 0.01$. (E) Evaluation of dystrophin-positive fibers using BrdU after systemic injection of PMO (320 mg/kg) into *mdx52* mice at 5 weeks. Triple immunohistochemical staining of cryosections in TA muscle of *mdx*52 mice for dystrophin, BrdU and DAPI. Data are representative of four independent experiments. Scale bar: 50 μm. (F) Statistical analysis of dystrophin-positive fibers using BrdU after systemic injection of PMO into *mdx52* mice. Fisher's exact test was used to test for the relationship between the BrdU and dystrophin expressions. $^{***}P < 0.001$.

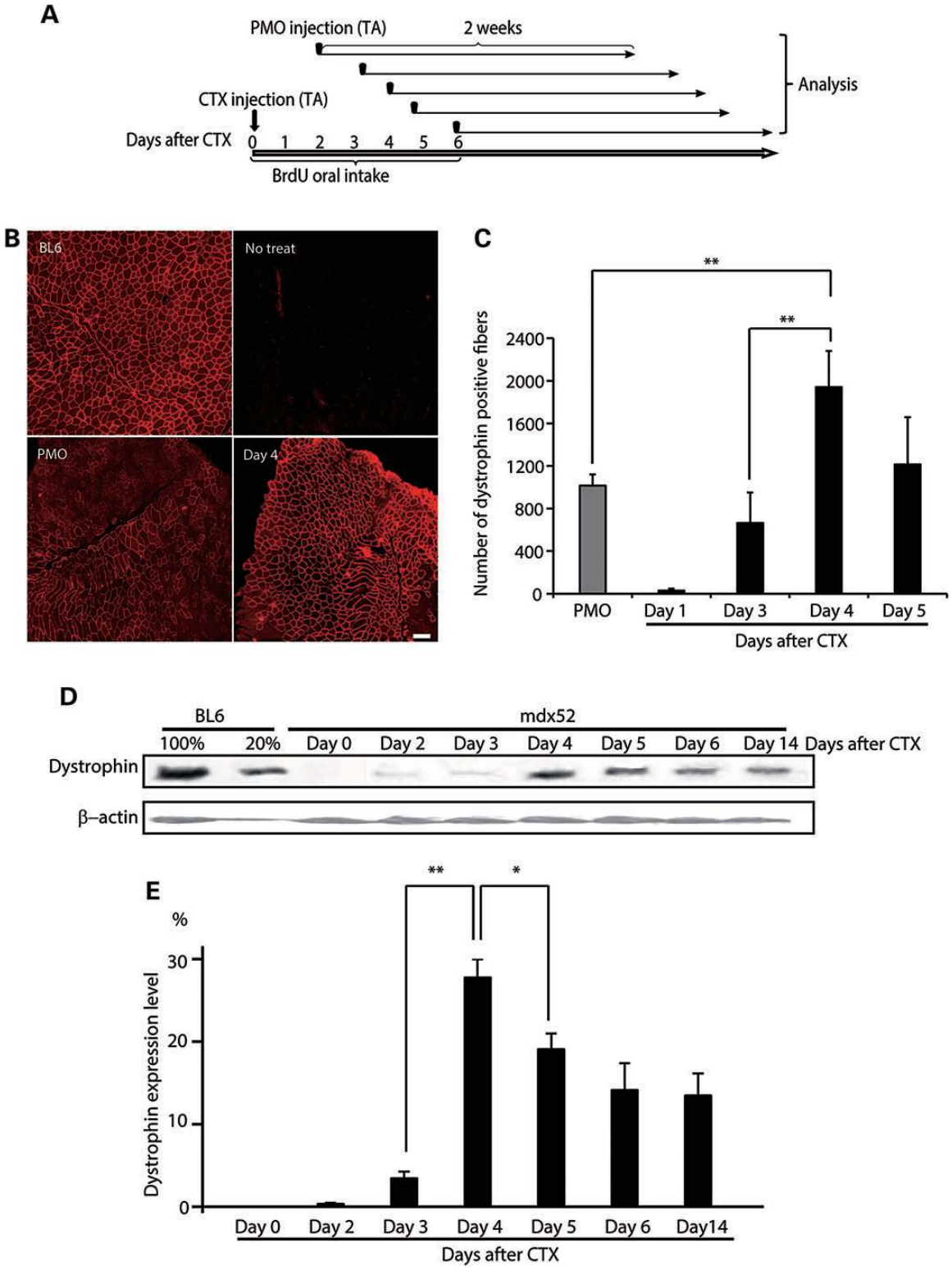

Figure 3. Evaluation of PMO entry into regenerating fibers during synchronized regeneration due to CTX injection in *mdx*52 mice. (A) Experimental model of the local intramuscular injection of CTX or PMO into *mdx*52 mice. Day 0 is defined as 5 weeks of *mdx*52 mice. CTX was injected into the TA muscles of *mdx*52 mice at Day 0. Between Day 0 and Day 6, PMO (400 μg/kg body weight) was injected into the CTX-injured TA muscles of *mdx*52 mice with oral administration of BrdU containing water (0.8 mg/ml). Analysis was performed 2 weeks after the PMO injection. (B) Immunohistochemical staining for dystrophin in the cryosections in TA muscles of *mdx*52 mice. Data are representative of six independent experiments. BL6: TA muscle from a WT C57/BL6. No treat: Untreated TA muscle from *mdx*52 mice. PMO: PMO-treated TA muscle from *mdx*52 mice. Day 4: PMO-treated CTX-injured TA muscle from *mdx*52 mice (CTX was injected 4 days before the PMO injection). Scale bar, 100 μm. (C) Percentage of dystrophin-positive fibers in CTX-injured TA muscle. The data ($n = 6$) are presented as mean ± SD. $^{**}P < 0.01$. (D) Western blotting for dystrophin in the CTX-injured TA muscles of *mdx*52 mice. Data are representative of four independent experiments. BL6 20%: TA muscle from a 20% extract of WT C57/BL6 mice. Anti-β-actin is used as loading controls. (E) Semi-quantitative analysis of dystrophin expression in TA muscles of *mdx*52 mice 2 weeks after the intramuscular injection of PMO. The data ($n = 4$) are presented as mean ± SD. $^{*}P < 0.05$ and $^{**}P < 0.01$.

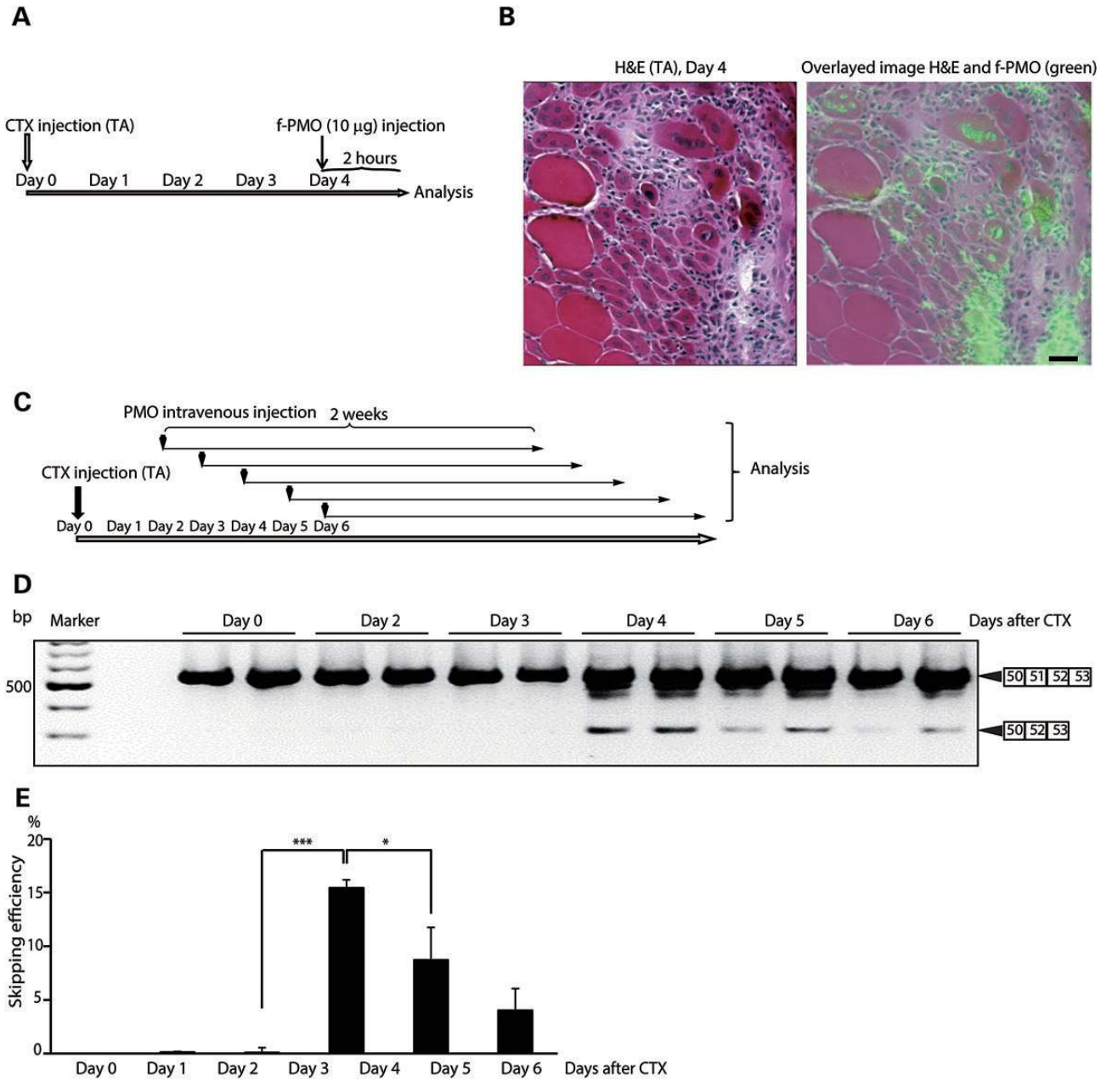

Figure 4. Skipping efficiency is increased dramatically when PMO is injected systemically at 4 days after CTX injury in WT mice. (A) Experimental model of the intramuscular injection of f-PMO into BL6 WT mice. f-PMO (400 μg/kg body weight) was injected into the CTX-injured TA muscles of *mdx*52 mice at Day 4 and the TA muscles analyzed 2 h after the injection of f-PMO. (B) Hematoxylin and eosin (H&E) staining (left) and immunofluorescence imaging of injured TA muscle for the detection of f-PMO (right). (C) Experimental model of the systemic intravenous injection of PMO into WT mice. Day 0 is defined as 5 weeks of WT mice. CTX was injected into the TA muscles of WT mice at Day 0. Between Day 0 and Day 6, PMO (320 mg/kg) was injected intravenously via tail vein into WT mice that had already received a CTX injection into TA muscles. RT–PCR analysis was performed 2 weeks after the PMO injection, respectively. (D) Detection of exon 51-skipped dystrophin mRNA by RT–PCR. Data are representative of four independent experiments. (E) Quantitative analysis by RT–PCR of exon 51 skipping by PMO. The percentages of skipped bands in each lane of (E) are shown. The data ($n = 4$) are presented as mean ± SD. $^{*}P < 0.05$ and $^{***}P < 0.001$.

muscles of 5-week-old WT mice, followed, 4 days later, by injection of f-PMO (400 μg/kg body weight) targeting the splice donor site of exon 51 into each TA muscle (Fig. 4A). Two hours later, the mice were killed and TA muscles were removed for microscopic analysis. Clearly, 4 days after CTX injection f-PMO had entered small-caliber-regenerated fibers of less than 35 μm, but not normal-caliber fibers with peripheral nuclei (Fig. 4B). Next, PMO 51Do (320 mg/kg) targeting the splice donor site of exon 51 was injected into the tail vein of 5-week WT mice 4 days after injection of CTX into their TA muscles (Fig. 4C). The mice were killed 2 weeks later and TA muscles were removed and analyzed by RT–PCR. The skipping ratios as evaluated by RT–PCR were 0.1, 0.3, 0.7, 15.3, 8.9 and 4.3% at Days 1, 2, 3, 4, 5 and 6 after the CTX injection,

respectively (Fig. 4D and E). These data show that small-caliber-regenerated fibers can take up PMO efficiently in WT mice with a strong preference at Days 4 and 5, the period of maximum myotube formation.

Efficient uptake of PMO by dystrophin-positive WT regenerated fibers at 4 days after CTX injection

We next analyzed the characteristics of eMHC-positive regenerated fibers induced by CTX injury (Fig. 5A). Four days after CTX intramuscular injection into TA muscles of 5-week-old WT mice, PMO 51Do (320 mg/kg) was injected via the tail vein. One hour later, the mice were killed and the TA muscles were removed for analysis by *in situ* hybridization with digoxigenin–alkaline phosphatase probes. This revealed that PMO 51Do was mainly present in the nucleus and to a lesser extent in the cytosol of small-caliber (<35 μm)-regenerated fibers, but was barely detectable in normal-caliber fibers with peripheral nuclei (Fig. 5B and C). Immunohistochemistry showed that fibers in which PMO 51Do was detected expressed dystrophin at the membrane (Fig. 5D and E).

In vitro evaluation of the period of uptake of PMO and 2′OMePS by mouse C2C12 myotubes

To examine the period of PMO uptake, we initially evaluated the expression level of dystrophin during C2C12 myoblasts differentiation and found the expression of dystrophin 24 h after the change of growth medium to differentiation medium by RT–PCR (Fig. 6A). Then, we transduced C2C12 myotubes with 10 μM PMO 51Do at 24, 48, 168 or 336 h after the medium change. We also tested the uptake period of 1 μM 2′OMePS, which is one of the commonly investigated oligonucleotides chemistries used for targeting the intraexonic site of exon 51. Undifferentiated C2C12 myoblasts after 10 μM PMO or 1 μM 2′OMePS were used as controls. After 48 h of incubation with PMO or 2′OMePS, the cells were collected and analyzed by RT–PCR (Fig. 6B and C). The skipping ratios of C2C12 myotubes after 10 μM PMO transfection were 32.6, 22.7, 9.8 and 6.1% after 24, 48, 168 or 336 h following the medium change, respectively (Fig. 6D). The skipping ratios after 1 μM 2′OMePS transfection over the same set of time periods were 22.9, 13.1, 2.5 or 1.2% after 24, 48, 168 or 336 h after the medium change, respectively (Fig. 6E). On the other hand, the skipping ratios of undifferentiated C2C12 myoblasts after 10 μM PMO or 1 μM 2′OMePS were 6.1 or 1.7%, respectively (Fig. 6D and E). These data support the idea that PMO or 2′OMePS is most efficiently taken up into muscle cells in the early stages of C2C12 myotube formation.

Proof of efficient PMO uptake by severely affected myofibers in dy^{3K}/dy^{3K} mice following systemic PMO injection

Finally, we performed PMO-mediated exon skipping for dy^{3K}/dy^{3K} mice, which are an animal model of laminin-α2 chain-deficient congenital muscular dystrophy and show severe dystrophic change with active muscle regeneration. Skipping exon 4 of the murine *Lama2* gene in dy^{3K}/dy^{3K} mice corrects the open reading frame and could lead to the production of a truncated laminin-α2 chain (Fig. 7A). We first identified effective AO sequences in dy^{3k}/dy^{3k} fibroblasts. We designed seven AO sequences targeting either exonic sequences or exon–intron junctions of the murine *Lama2* exon 4 (Fig. 7B; sequences in Table 3). We then transfected one or two of the seven AOs (10 μM in total) into dy^{3k}/dy^{3k} fibroblasts (17). After 48 h incubation, we analyzed RNA fractions by RT–PCR using the primers described in Supplementary Material, Figure S6. Among the AOs examined, PMO 4B plus 4D were shown to be capable of inducing exon 4 skipping at a level approaching 80%, the highest among the combinations that we examined by RT–PCR (Fig. 7C and D). 4B and 4D were designed to target the exonic sites of exon 4. We therefore injected the combination of two AOs (400 μg/kg body weight) into the TA muscles of dy^{3K}/dy^{3K} mice at age 10 days. Fifteen days later, TA muscles were obtained and analyzed by RT–PCR and immunohistochemistry. We found by RT–PCR that 4B plus 4D could induce exon 4 skipping (Fig. 8A). We confirmed correct exon 4 skipping by direct sequencing of the RT–PCR products (Fig. 8B). Moreover, up to 20% of fiber membranes were laminin-α2 positive by immunohistochemistry (Fig. 8C). After intraperitoneal injection (150 mg/kg in total) of the 2-PMO combination into dy^{3K}/dy^{3K} mice at postnatal at age 10 days, we found that 4B plus 4D could induce exon 4 skipping by RT–PCR (Fig. 8D). Our study results showed a trend toward improvement in life span of PMO-treated dy^{3k}/dy^{3k} mice compared with saline-treated dy^{3K}/dy^{3K} mice (Fig. 8E). These data suggest the potential of PMO-mediated therapy targeting myotubes for MDC1A.

DISCUSSION

We demonstrated here that PMO can be taken up into dystrophin and eMHC-positive regenerated fibers in WT mice. We also showed that PMO and 2′OMePS could be taken up into C2C12 myoblasts in the early stages of C2C12 myotube formation. These results suggest that we can apply PMO- or 2′OMePS-mediated therapy targeting myotube formation to other muscular diseases. To confirm our hypothesis, we finally showed the restoration of laminin-α2 chain expression by exon 4 skipping against the *Lama2* gene and a prolonged lifespan after intraperitoneal injection of PMO into dy^{3K}/dy^{3K} mice, which is a model of MDC1A (16).

PMO, which has a neutral chemistry, provides greatly decreasing the chance of catastrophic off-target antisense effects, and minimizes interactions with cationic moieties of proteins (11,18–21). These characteristics of PMO contribute to their extremely low toxicity and suitability for use in human. PMO is also being used extensively as a tool for selective inhibition of gene expression in cell culture models (22).

At present, the changes of membrane permeability of dystrophin-deficient muscle membrane, so-called ‘leaky membrane hypothesis’, facilitating a route of entry for the PMO into myofibers, are a favored explanation for PMO uptake (23–25). This hypothesis is based on the clinical evidence that dystrophin-deficient muscle fibers are prone to be injured by contraction and that the injury causes leakage of soluble cytoplasmic proteins such as creatine kinase (26,27). In addition, it is reported that intravenously delivered PMO shows very poor delivery to normal muscle, while dystrophin-deficient muscle

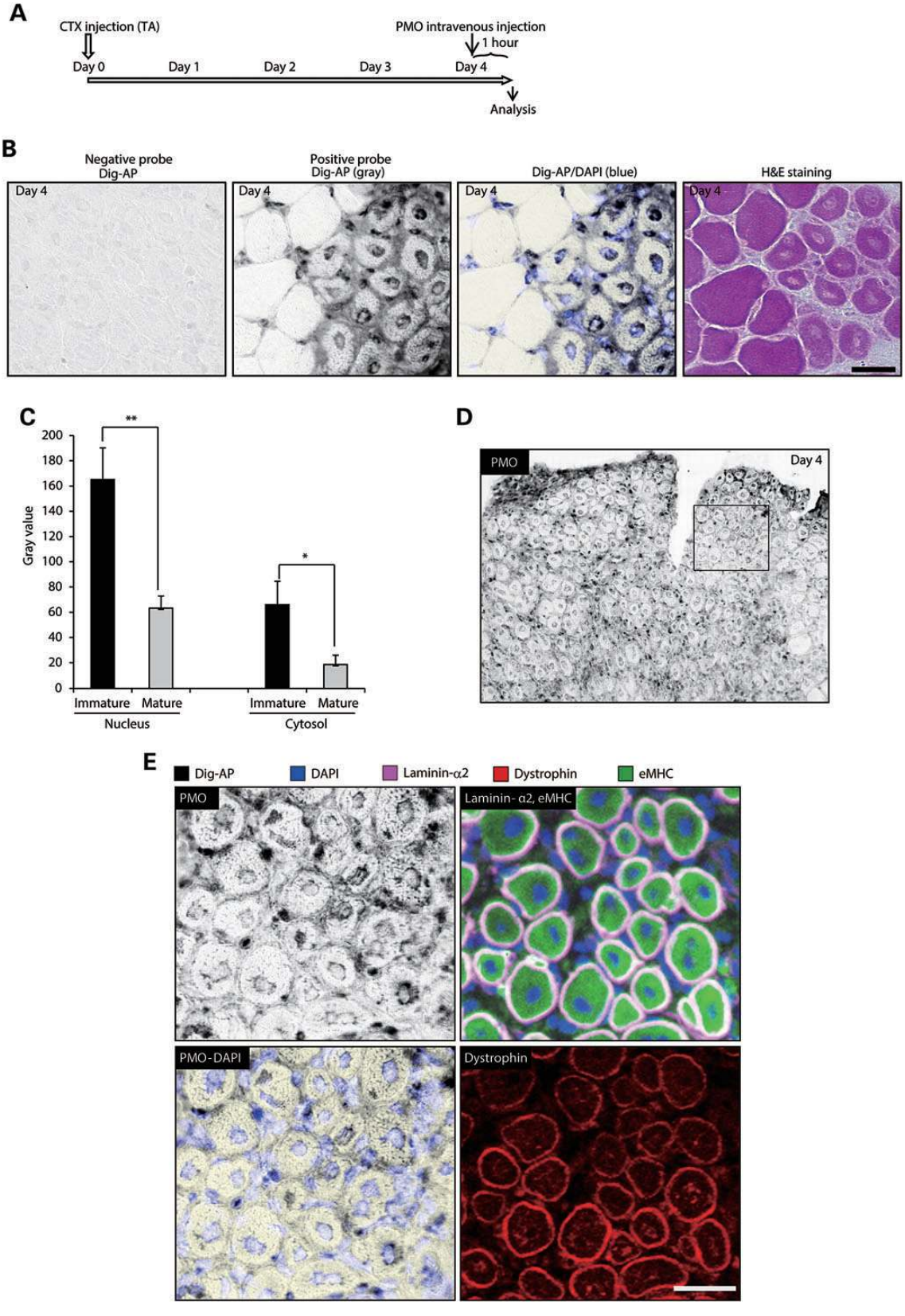

Figure 5. Detection of 25-mer PMO in myofibers on TA muscle cryosections by *in situ* hybridization. (A) Experimental model of the systemic intravenous injection of PMO into BL6 WT mice. Day 0 is defined as 5 weeks of WT mice. Cardiotoxin (CTX) was injected into the TA muscles of WT mice at Day 0. At Day 4, PMO (320 mg/kg) was injected intravenously via tail vein into the WT mice and TA muscles collected 1 h after the injection. (B) *In situ* hybridization for the direct detection of PMO

or intramuscular injection in normal muscle shows good delivery (28). Further, Evans blue, a low molecular-weight diazo dye which has a very high affinity for serum albumin, does not cross into skeletal muscle fibers in normal mice but *mdx* mice, a dystrophin-deficient animal model for DMD, show significant Evans blue accumulation in skeletal muscle fibers (29,30).

However, the hydrophobic plasma membrane constitutes an almost insurmountable barrier around muscle fibers, resulting in poor delivery of the neutral PMO, and preventing optimization of PMO-mediated therapy for DMD or other muscular dystrophies (31,32). To overcome this delivery issue with PMO, recent developments using cell-penetrating peptide-conjugated PMO, where a short cationic peptides that penetrate cells by interacting with the negatively charged plasma membrane, may become an effective strategy for reducing both dose levels and administration frequencies (33–36). But we still face issues of off-target effects or high toxicity in humans because of the nonspecific delivery-facilitated properties and the facilitated interactions with other proteins (37–40). Therefore, it is important to understand the detailed mechanisms of PMO entry into muscle fibers to improve the poor delivery of PMO and optimize it as a therapeutic intervention for DMD or other muscular diseases.

In this study, we found that exon 51 skipping was induced dose dependently in *mdx*52 mice but that no skipping was induced in WT mice after systemic injection of PMO (640 mg/kg). This finding conforms the 'leaky membrane hypothesis'. However, PMO was most efficiently taken up into eMHC-positive regenerating fibers at 4 days following CTX injection into TA muscles, which express dystrophin at the muscle plasma membrane in WT mice. The degeneration–regeneration process induced by CTX injection was well documented as follows: after CTX injection, satellite cell proliferation occurs within 2 days, myogenic differentiation is initiated within 3 days, new myotube formation is evident within 5 days and muscle architecture is largely restored within 10 days (41). Taken together, our *in vivo* study by CTX injection suggests PMO uptake is more prominent during stages from myogenic differentiation to myotube formation than cell proliferation stage. We also showed that PMO and 2′OMePS is taken up efficiently in the early stages of C2C12 myotube formation. These data suggest that the uptake mechanism is not simply attributable to a change in membrane permeability but also involves an unknown mechanism in the early stages of C2C12 myotube formation. It is reported that PMO internalization in uptake-permissive cells is specific, saturable and energy dependent, suggesting a receptor-mediated mechanism (22). These data suggest that immature regenerated fibers, which are called myotubes, could take up PMO more efficiently than mature fibers. In consequence, we confirmed that there is already a leaky gateway into dystrophin-deficient muscle fibers. But more importantly, these findings provide a conceptual advance in that it supports the idea that PMO entry into muscle fibers is dependent on a developmental stage in myogenesis rather than on an intrinsic defect in the dystrophin-deficient muscle membrane: the 'leaky-membrane' hypothesis. As such it provides a platform for developing PMO-mediated therapies for a variety of muscular disorders, such as MDC1A, that involve active muscle regeneration.

To test the potential of PMO treatment targeting myotube formation, we used the dy^{3K}/dy^{3K} mouse which is a model of MDC1A. The dy^{3K}/dy^{3K} mice, with a pMC1neo polyA+ cassette in exon 4 of the *Lama2* gene, are a null mutant for the laminin-α2 chain which is a major component of basal lamina in skeletal muscle and the peripheral nervous system (16). In man, the laminin-α2 chain consists of six domains (I–VI) and exon 4 of the *LAMA2* gene encodes a part of domain VI, which are predicted to form N-terminal globular (LN) structures (Supplementary Material, Fig. S7A) (42). The LN structures are essential for laminin aggregation into supramolecular networks and consequently for incorporation into basement membranes, thus mutations in this structures reduce the capacity of polymer formation (43). Another merosin-deficient mouse, the dy^{2J}/dy^{2J} mouse, harbors a mutation in the LN structures which leads only to slightly reduced expression of a laminin-α2 chain partially lacking these structures and thus displays a relatively mild muscular dystrophy and peripheral neuropathy (44). Therefore, we hypothesized that PMO-mediated exon 4 skipping could act to rescue dy^{3K}/dy^{3K} mice. In this study, we successfully confirmed the recovery of laminin-α2 chain by skipping of the mutated exon 4. Our data suggest that PMO, which was taken up into muscle fibers, may induce exon 4 skipping in dy^{3K}/dy^{3K} mice. More importantly, PMO-mediated exon 4 skipping has a real potential to become an effective therapy for MDC1A, since two nonsense mutations in exon 4 such as 547G > ANN166X and 677C > T/210X can cause MDC1A (45). Furthermore, half of the patients with congenital muscular dystrophy in European populations have mutations of the *LAMA2* gene (42), our data could offer a hope to patients struggling with the disease.

In conclusion, PMO or 2′OMePS is taken up preferentially into mouse muscle cells during myotube fusion. Our results can provide a platform for developing PMO-mediated therapies for a variety of muscular disorders, such as MDC1A, that involve active muscle regeneration. They also directs us to interrogate myogenic developmental mechanisms as opposed to defects in membrane function in mature muscle fibers for clues as to how to facilitate PMO delivery in other myopathies.

MATERIALS AND METHODS

Animals

Exon 52-deficient, X chromosome-linked muscular dystrophy (*mdx*52) mice were produced by a gene-targeting strategy and maintained at our facility (15). The mice have been backcrossed to the C57BL/6J WT strain for more than eight generations. Male *mdx*52 mice ages 3–32 weeks and WT mice age 5 weeks were used in this study.

on frozen TA muscle cryosections 1 h after systemic intravenous injection of the PMO into WT mice that had received CTX injection at Day 0; H&E, hematoxylin and eosin staining. (C) Quantitative analysis of the intensity of positive probe signal in muscle fibers 1 h after the PMO injection. The data ($n = 4$) are presented as mean ± SD. $^{*}P < 0.05$ and $^{***}P < 0.001$. (D and E) *In situ* hybridization for the direct detection of PMO on TA muscle cryosections. Data are representative of four independent experiments. (E) Enlarged view of rectangle area in (D). Staining of serial cryosections with anti-eMHC antibody (green), anti-laminin α2 chain antibody (pink), DAPI (blue) and anti-dystrophin antibody (red). Dig-AP: digoxigenin-alkaline phosphatase.

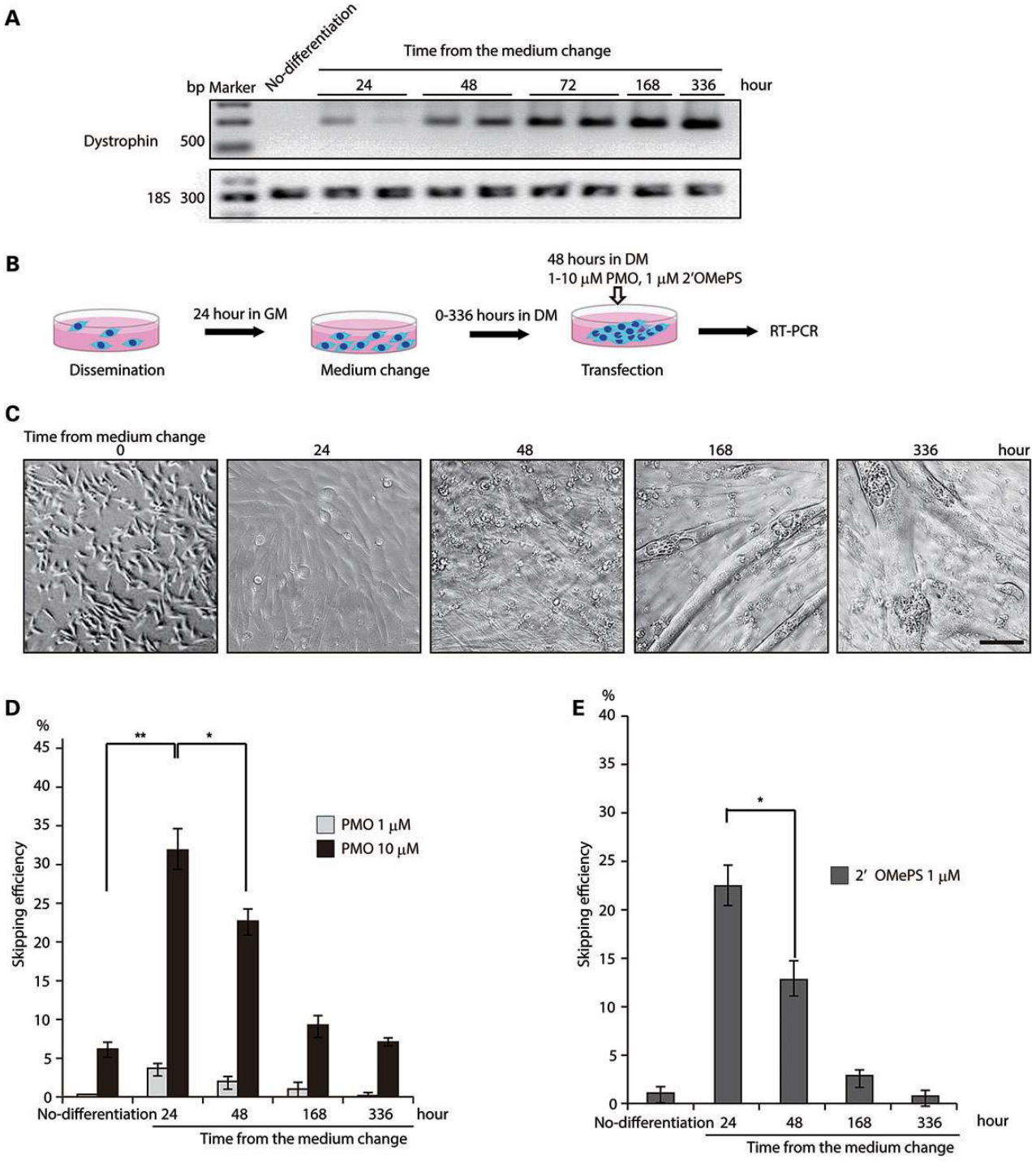

Figure 6. Evaluation of PMO or 2′OMePS uptake by C2C12 myoblasts in the differentiation process. (A) Detection of dystrophin mRNA by RT–PCR during C2C12 myoblasts differentiation. Differentiating C2C12 myoblasts were examined after a 24-, 48-, 168- or 336-h incubation and analyzed by RT–PCR. Representative data are shown. Data are representative of four independent experiments. (B) Experimental model of PMO or 2′OMePS transfection into C2C12 myoblasts. Differentiating C2C12 myoblasts were examined after a 48-h incubation with a PMO or 2′OMePS at a final concentration of 10 or 1 μM, respectively. (C) Pictures of C2C12 myoblasts at 24 h, 48 h, 7 days or 14 days after the switch from a growth medium to a differentiation medium. (D) Quantitative analysis of dystrophin expression by RT–PCR after the PMO transfection into C2C12 myoblasts is shown. The data ($n = 6$) are presented as mean ± SD. $^{**}P < 0.01$. (E) Exon 51 skipping by appropriate 2′OMePS can restore the reading frame of dystrophin in the *mdx*52 mouse. Quantitative analysis of dystrophin expression by RT–PCR after the 2′OMePS transfection into C2C12 myoblasts is shown. The data ($n = 3$) are presented as mean ± SD. $^{*}P < 0.05$.

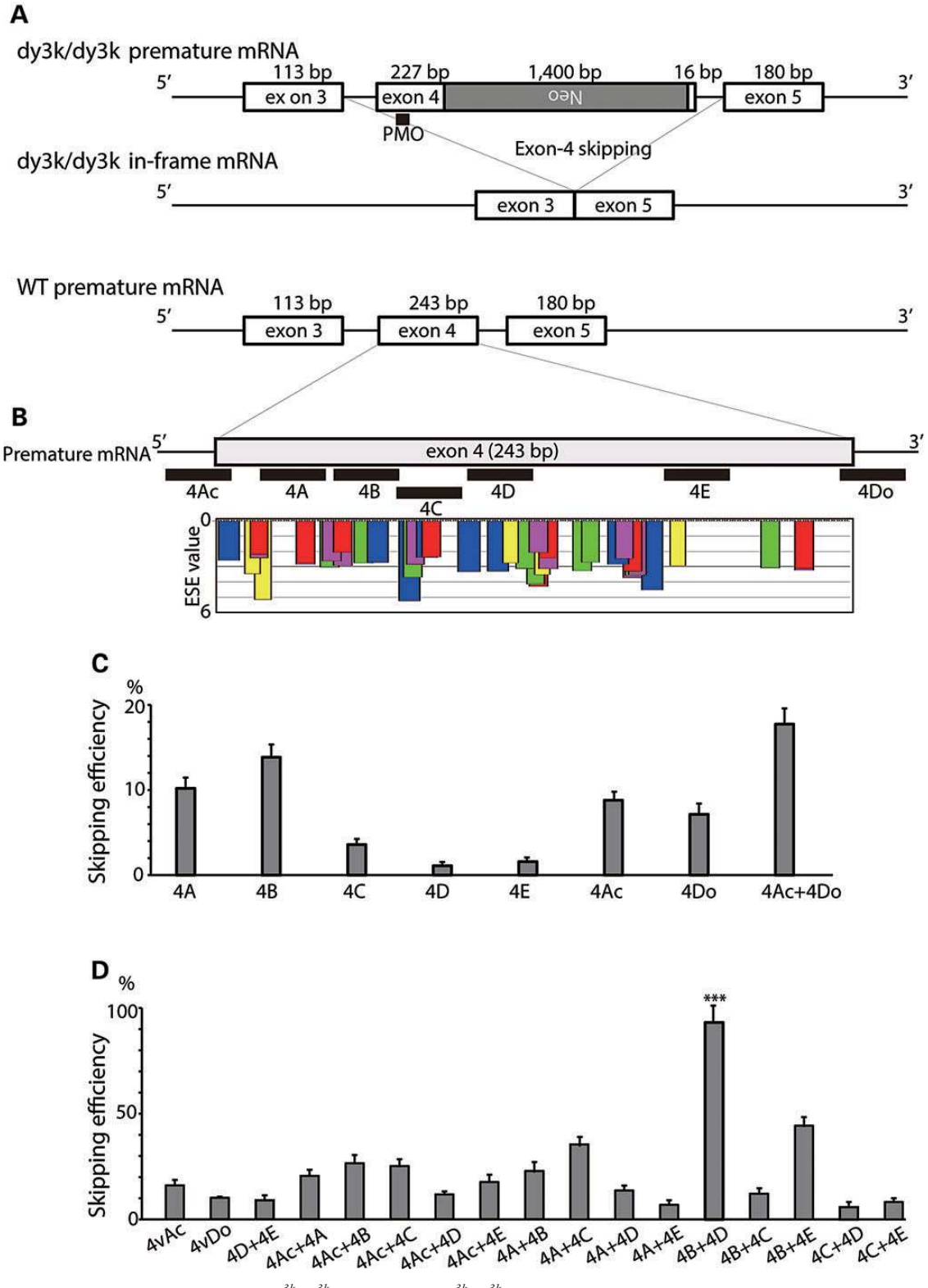

Figure 7. *In vitro* evaluation of the PMO sequences in dy^{3k}/dy^{3k} fibroblasts. (A) dy^{3k}/dy^{3k} mice have a pMC1neo polyA+ cassette (*Neo*) in exon 4 of the *Lama2* gene in the reverse direction, leading to out-of-frame products. Exon 4 skipping with PMO (black line) restores the reading frame of *Lama2* mRNA. (B) Schematic outline of the PMO targeting exon 4 of murine *Lama2* mRNA. Each PMO targets either an exonic splicing enhancer (ESE) or the 5′ or 3′ splice site, indicated by black lines. The certainties of exonic splicing enhancer sites according to ESEfinder 3.0 (46) are indicated by colored boxes. Candidates for splicing enhancer-binding proteins are shown: red, SF2/ASF; purple, SF2/ASF (IgM-BRCA1); blue, SC35; green, SRp40; yellow, SRp55. Quantitative analysis by RT–PCR of exon 4 skipping by 7 different single PMOs (C) and by 15 different combinations of two PMOs (D) in C2C12 myotubes. The data ($n = 5$) are presented as mean ± SD.

Table 3. AO sequences against exon 4 of the *Lama2* gene of mice used in this study

Name	Position	Sequence
4Ac	−19+6	GAACACCTGATGATGGGTGACAAAA
4Do	+5−20	ATGCAGCTTTTGATCTTACCTCTC
4A	+17+41	GAATTGGCTGCCTTCACAATTACGT
4B	+45+69	TTCCAAAATCCAGTTTCCAGGCCGA
4C	+69+93	GTACTCCACGTCATCCAGGGAACGT
4D	+96+120	TGTCACCGCATGATACTGCCAGGGT
4E	+171+195	GACCTCATCATCTTTGGCGTAGGAT

Heterozygous *Lama2* gene-targeted dy^{3K} mice, which have a pMC1neo polyA+ cassette in exon 4 of the *Lama2* gene, were maintained in our animal facility. The heterozygous mice were interbred to obtain homozygous dy^{3K}/dy^{3K} mice. Genotyping of the *Lama2* deficiency was performed by PCR on tail genomic DNA. The PCR primers for the WT *Lama2* allele and the mutant allele are described in Table 4. Mice showing WT *Lama2*-negative and neo-positive PCR products were defined as *Lama2* homodeficient (dy^{3k}/dy^{3k}).

All experimental protocols in this study were approved by the Experimental Animal Care and Use Committee of the National Institute of Neuroscience, National Center of Neurology and Psychiatry, Japan.

BrdU injections

BrdU (Sigma-Aldrich, St. Louis, MO, USA) was dissolved in PBS (Gibco, Paisley, UK) and stored at 3 mg/ml at −20°C. Mice were treated with 0.8 mg/ml BrdU in their drinking water for 7 days. BrdU solution was prepared in sterile water, protected from light exposure and changed daily.

Antisense sequences and delivery methods

AO for targeted skipping of exon 51 during dystrophin pre-mRNA splicing in mice were designed to anneal to the 3′ splice site (51Do) according to our previously published report (5). The sequence was synthesized using a PMO, f-PMO (Gene Tools, LLC, Philomath, OR, USA) or 2′OMePS (Operon Biotechnologies, Tokyo, Japan). Primers for RT–PCR and sequencing analysis were synthesized by Operon Biotechnologies and are listed in Table 4.

For local studies, PMO or 2′OMePS at a dose of 400 μg/kg body weight was injected into each TA muscle of *mdx*52 mice. Muscles were obtained 2 weeks after the intramuscular injection and analyzed by RT–PCR and the cryosections by immunohistochemistry. For the systemic studies, a dose of 80–640 mg/kg PMO in 100 μl of saline or 100 μl saline was injected into the tail vein of *mdx*52 mice or WT mice, singly, and mice were examined 2 weeks after the injection. Muscles were dissected immediately, snap-frozen in liquid nitrogen-cooled isopentane and stored at −80°C for RT–PCR, immunohistochemistry and western blotting.

AO transfection

In the 2% differentiation medium, C2C12 myotubes were incubated up to 14 days. We then transfected PMO or 2′OMePS at the final concentration of 10 or 1 μM, respectively, into C2C12 myotubes without any transfection agents and incubated them for 48 h.

RT–PCR and sequencing of cDNA

Total RNA was extracted from cells or frozen tissue sections using TRIzol (Invitrogen, Carlsbad, CA, USA). Two hundred nanograms of total RNA template were used for RT–PCR with a QuantiTect Reverse Transcription Kit (Qiagen, Crawley, UK) according to the manufacturer's instructions. The cDNA product (0.5 μl) was then used as the template for PCR in a 20-μl reaction with 0.1 units of TaqDNA polymerase (Qiagen). The reaction mixture comprised 10× PCR buffer (Roche, Basel, Switzerland), 10 mM of each dNTP (Qiagen) and 10 μM of each primer. The primer sequences were Ex50F 5′-TTTACTTCGGGAGCTGAGGA-3′ and Ex53R 5′-ACCTG TTCGGCTTCTTCCTT-3′ for amplification of cDNA from exons 50 to 53. The cycling conditions were 95°C for 4 min, then 35 cycles of 94°C for 0.5 min, 60°C for 0.5 min, 72°C for 0.5 min and finally 72°C for 7 min. The intensity of PCR bands was analyzed using ImageJ software (http://rsbweb.nih.gov/ij/), and skipping efficiency was calculated by using the following formula: [(the intensity of skipped band)/(the intensity of skipped band + the intensity of unskipped band)]. After the resulting PCR bands were extracted using a gel extraction kit (Qiagen), direct sequencing of PCR products was performed by the Biomatrix Laboratory Co., Ltd. (Chiba, Japan).

Immunohistochemistry and hematoxylin and eosin staining

At least ten 8-μm cryosections were cut from flash-frozen muscles at 100-μm intervals. The serial sections were stained with polyclonal rabbit antibody P7 against the dystrophin rod domain (a gift from Dr. Qi-Long Lu, Carolinas Medical Center, Charlotte, NC, USA), monoclonal mouse antibody developmental MHC (Leica Biosystems, Newcastle Upon Tyne, UK), anti-laminin-α2 monoclonal rat antibody 4H8-2 (Abcam, Cambridge, UK) and anti-laminin polyclonal rabbit antibody L9393 (Sigma-Aldrich). Alexa-488 or 568 (Molecular Probes, Cambridge, UK) was used as a secondary antibody. DAPI containing a mounting agent (Vectashield; Vector Laboratories, Burlingame, CA, USA) was used for nuclear counterstaining. The maximum number of dystrophin-positive fibers in one section was counted, and the TA muscle fiber sizes were evaluated using a BZ-9000 fluorescence microscope (Keyence, Osaka, Japan). Hematoxylin and eosin staining was performed using Harris hematoxylin and eosin.

Western blotting

Muscle protein from cryosections was extracted with lysis buffer as described previously (5). A total of 2–20 μg protein was loaded onto a 5–15% XV Pantera Gel (DRC, Tokyo, Japan). The samples were transferred onto an Immobilon polyvinylidene fluoride membrane (Millipore, Billerica, MA, USA) by semi-dry blotting at 5 mA/mm^2 for 1.5 h. The membrane was incubated with the C-terminal monoclonal antibody Dys2 (Leica Biosystems, Newcastle Ltd.) at room temperature for 1 h. The bound primary antibody was detected by horseradish

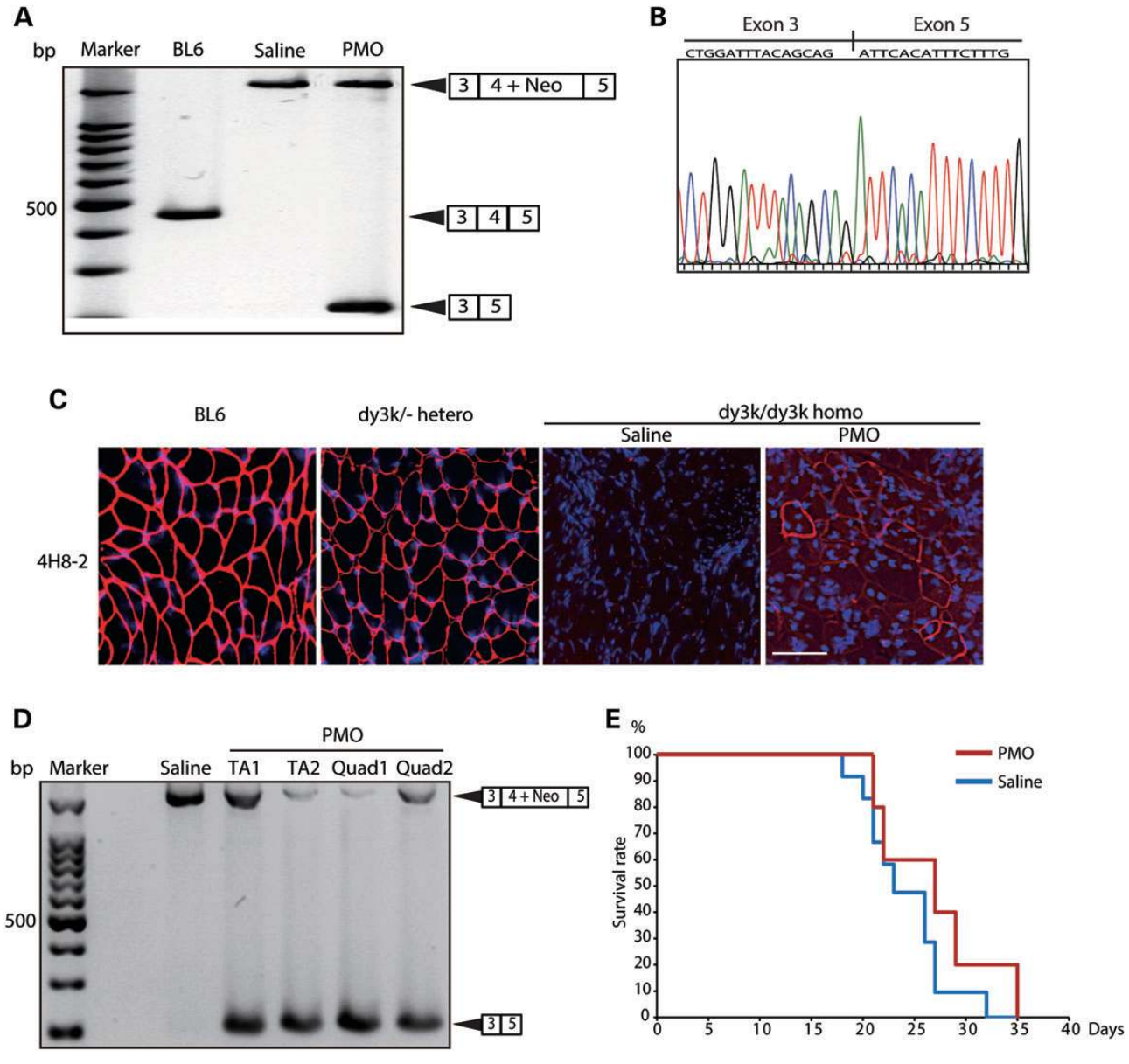

Figure 8. Recovery of laminin-α2 chain expression at the basement membrane of TA muscle in dy^{3k}/dy^{3k} mice following systemic PMO injection. (A) PMO (400 μg/kg body weight) was injected into the TA muscles of dy^{3k}/dy^{3k} mice at 5 days and RT–PCR or immunohistochemistry was performed 15 days after the injection, respectively. Effectiveness of exon 4 skipping detected by RT–PCR. Data are representative of four independent experiments. BL6: TA muscle from a WT C57/BL6. Saline: Saline-treated TA muscle from dy^{3k}/dy^{3k} mice at 10 days. PMO: Treated TA muscle from dy^{3k}/dy^{3k} mice at 25 days. $^{***}P < 0.001$. (B) Confirmation of correct exon-4 skipping by direct sequencing of the PCR products. Sequencing of the most intense band shows the exon 4-skipped *Lama2* mRNA sequence. (C) Immunohistochemical staining for laminin-α2 chain in the TA muscle. Data are representative of four independent experiments. BL6: TA muscle from a WT C57/BL6. Saline: Saline-treated TA muscle from dy^{3k}/dy^{3k} mice. PMO: PMO-treated TA muscle from dy^{3k}/dy^{3k} mice. Scale bar: 100 μm. (D and E) PMO (150 mg/kg in total) was injected intraperitoneally into the dy^{3k}/dy^{3k} mice at postnatal 4–6 days. Effectiveness of exon 4 skipping detected by RT–PCR (D). Kaplan–Meier survival analysis of saline-treated ($n = 12$) or PMO-treated dy^{3k}/dy^{3k} mice ($n = 5$) is shown (E). Quad: quadriceps. TA1 and Quad1: TA and Quad muscle from dy^{3k}/dy^{3k} mice no. 1. Quad2: TA and Quad muscle from dy^{3k}/dy^{3k} mice no. 2.

peroxidase-conjugated goat anti-mouse IgG (Cedarlane, Burlington, ON, USA) and SuperSignal chemiluminescent substrate (Pierce, Rockford, IL, USA). Anti-β-actin antibody was used as a loading control. The signal intensity of detected bands of the blots was quantified using ImageJ software and normalized to the loading control.

In situ hybridization

DNA probes with 3′-DIG tailing for *in situ* hybridization were synthesized by Nihon Gene Research Laboratories Inc. (Sendai, Japan) and are listed in Table 2. At least ten 10-μm cryosections were cut from flash-frozen muscles. The sections were

Table 4. Primer pairs for the *Dmd* or *Lama2* gene of mice used in this study

(i) Primer pair for the *Dmd* gene
Forward primer: 5′-TTTACTTCGGGAGCTGAGGA-3′
Reverse primer: 5′- ACCTGTTCGGCTTCTTCCTT-3′
(ii) Primer pair for the *Lama2* gene
Forward primer: 5′-GGTGGCAGAGTCCCAGTATC-3′
Reverse primer: 5′-CGATTTCTCTGGGGTCTTTG-3′
(iii) Primer pair for the WT *Lama2* allele
Forward primer: 5′-CCAGATTGCCTACGTAATTG-3′
Reverse primer: 5′-CCTCTCCATTTTCTAAAG-3′
(iv) Primer pair for the mutant *Lama2* allele
Forward primer: 5′-CTTGGGTGGAGAGGCTATTC-3′
Reverse primer: 5′-AGGTGAGATGACAGGAGATC-3′

fixed in 4% paraformaldehyde for 30 min and dehydrated for 16 h at 42°C. The sections were incubated in HCl (0.2 N) for 20 min and subjected to pretreatment with proteinase K (1 μg/ml) for 15 min at 37°C. The sections were fixed in 4% paraformaldehyde for 5 min at room temperature and then incubated in glycine (10 mg/ml) for 15 min. Next, sections were subjected to incubation for 2 h in prehybridization solution: 40% deionized formamide and 4 × SSC buffer. The sections were hybridized for 14 h at 30°C in a hybridization solution containing 3 μg/ml of digoxigenin-labeled probe. The sections were then washed sequentially for 60 min with 2 × SSC, 1 × SSC and 0.5 × SSC. The final wash was with 0.1 × SSC for 40 min. For detection of digoxigenin-labeled probe, anti-digoxigenin–alkaline phosphatase (Roche) and NBT/BCIP Stock Solution (Roche) were used according to the manufacturer instructions. After the development, slides were counterstained with hematoxylin/eosin. The *in situ* hybridization solution contained 40% formamide (Sigma-Aldrich), 10 mM Tris (pH 7.5), 1 × Denhardt's solution, 1 mM EDTA, 20% dextran sulfate (Pharmacia, Basking Ridge, NJ, USA), 5 M NaCl, 0.25 mg of salmon DNA and 0.25 mg of yeast tRNA.

Statistical analysis

Statistical differences were assessed by one-way analysis of variance with differences among the groups assessed by a Tukey's comparison or Fisher's exact test. All data are reported as mean values ± SD or SEM. The level of significance was set at $P < 0.05$.

SUPPLEMENTARY MATERIAL

Supplementary Material is available at *HMG* online.

ACKNOWLEDGEMENTS

The authors thank Yuko Suzuki and Michihiro Imamura for insightful discussions about this study. We thank Takashi Saito, Jun Tanihata, Yuko-Motohashi Shimizu, Satoru Masuda, Hayashiji Nozomi and Ryoko Nakagawa for useful discussions and technical assistance. We also thank Kenji Kuwabara, Kazushi Takagaki, Satoru Sonoke, Kaoru Fujiwara and other members of Nippon Shinyaku Co Ltd.

Conflict of Interest statement. None declared.

FUNDING

This work was supported by an Intramural Research Grant (22-5) for Neurological and Psychiatric Disorders of the National Center of Neurology and Psychiatry, Health and Labour Sciences Research Grants for Translation Research (H21-Translational Research-011), Health and Labour Sciences Research Grants for Translation Research (H21-Clinical Research-015), Comprehensive Research on Disability Health and Welfare (H23-Neuromuscular Disease-005) from the Ministry of Health, Labour, and Welfare of Japan and MRC Confidence in Concept Award (CiC17).

REFERENCES

1. Hoffman, E.P., Brown, R.H. and Kunkel, L.M. (1987) Dystrophin: the protein product of the Duchenne muscular dystrophy locus. *Cell*, **51**, 919–928.
2. Monaco, A.P., Bertelson, C.J., Liechti-Gallati, S., Moser, H. and Kunkel, L.M. (1988) An explanation for the phenotypic differences between patients bearing partial deletions of the DMD locus. *Genomics*, **2**, 90–95.
3. Matsuo, M., Masumura, T., Nishio, H., Nakajima, T., Kitoh, Y., Takumi, T., Koga, J. and Nakamura, H. (1991) Exon skipping during splicing of dystrophin mRNA precursor due to an intraexon deletion in the dystrophin gene of Duchenne muscular dystrophy Kobe. *J. Clin. Invest.*, **87**, 2127–2131.
4. Wood, M.J.A. (2010) Toward an oligonucleotide therapy for Duchenne muscular dystrophy: a complex development challenge. *Sci. Transl. Med.*, **2**, 25ps15.
5. Aoki, Y., Nakamura, A., Yokota, T., Saito, T., Okazawa, H., Nagata, T. and Takeda, S. (2010) In-frame dystrophin following exon 51-skipping improves muscle pathology and function in the exon 52-deficient mdx mouse. *Mol. Ther.*, **18**, 1995–2005.
6. Aoki, Y., Yokota, T., Nagata, T., Nakamura, A., Tanihata, J., Saito, T., Duguez, S.M.R., Nagaraju, K., Hoffman, E.P., Partridge, T. *et al.* (2012) Bodywide s kipping of exons 45–55 in dystrophic mdx52 mice by systemic antisense delivery. *Proc. Natl. Acad. Sci. USA*, **109**, 13763–13768.
7. Yokota, T., Lu, Q.-L., Partridge, T., Kobayashi, M., Nakamura, A., Takeda, S. and Hoffman, E. (2009) Efficacy of systemic morpholino exon-skipping in Duchenne dystrophy dogs. *Ann. Neurol.*, **65**, 667–676.
8. Lu, Q.L., Rabinowitz, A., Chen, Y.C., Yokota, T., Yin, H., Alter, J., Jadoon, A., Bou-Gharios, G. and Partridge, T. (2005) Systemic delivery of antisense oligoribonucleotide restores dystrophin expression in body-wide skeletal muscles. *Proc. Natl. Acad. Sci. USA*, **102**, 198–203.
9. Cirak, S., Arechavala-Gomeza, V., Guglieri, M., Feng, L., Torelli, S., Anthony, K., Abbs, S., Garralda, M.E., Bourke, J., Wells, D.J. *et al.* (2011) Exon skipping and dystrophin restoration in patients with Duchenne muscular dystrophy after systemic phosphorodiamidate morpholino oligomer treatment: an open-label, phase 2, dose-escalation study. *Lancet*, **378**, 595–605.
10. Goemans, N.M., Tulinius, M., Van den Akker, J.T., Burm, B.E., Ekhart, P.F., Heuvelmans, N., Holling, T., Janson, A.A., Platenburg, G.J., Sipkens, J.A. *et al.* (2011) Systemic administration of PRO051 in Duchenne's muscular dystrophy. *N. Engl. J. Med.*, **364**, 1513–1522.
11. Arora, V., Devi, GR. and Iversen, PL. (2004) Neutrally charged phosphorodiamidate morpholino antisense oligomers: uptake, efficacy and pharmacokinetics. *Curr. Pharm. Biotechnol.*, **5**, 431–439.
12. Ghosh, C. and Iversen, P.L. (2000) Intracellular delivery strategies for antisense phosphorodiamidate morpholino oligomers. *Antisense Nucleic Acid Drug Dev.*, **10**, 263–274.
13. Petrof, B.J., Shrager, J.B., Stedman, H.H., Kelly, A.M. and Sweeney, H.L. (1993) Dystrophin protects the sarcolemma from stresses developed during muscle contraction. *Proc. Natl. Acad. Sci. USA*, **90**, 3710–3714.
14. McArdle, A., Edwards, R.H. and Jackson, M.J. (1994) Time course of changes in plasma membrane permeability in the dystrophin-deficient mdx mouse. *Muscle Nerve*, **17**, 1378–1384.

15. Araki, E., Nakamura, K., Nakao, K., Kameya, S., Kobayashi, O., Nonaka, I., Kobayashi, T. and Katsuki, M. (1997) Targeted disruption of exon 52 in the mouse dystrophin gene induced muscle degeneration similar to that observed in Duchenne muscular dystrophy. *Biochem. Biophys. Res. Commun.*, **238**, 492–497.
16. Miyagoe, Y., Hanaoka, K., Nonaka, I., Hayasaka, M., Nabeshima, Y., Arahata, K. and Takeda, S. (1997) Laminin alpha2 chain-null mutant mice by targeted disruption of the Lama2 gene: a new model of merosin (laminin 2)-deficient congenital muscular dystrophy. *FEBS Lett.*, **415**, 33–39.
17. Saito, T., Nakamura, A., Aoki, Y., Yokota, T., Okada, T., Osawa, M. and Takeda, S. (2010) Antisense PMO found in dystrophic dog model was effective in cells from Exon 7-deleted DMD patient. *PLoS ONE*, **5**, 8.
18. Amantana, A. and Iversen, PL. (2005) Pharmacokinetics and biodistribution of phosphorodiamidate morpholino antisense oligomers. *Curr. Opin. Pharmacol.*, **5**, 550–555.
19. Hudziak, R.M., Barofsky, E., Barofsky, D.F., Weller, D.L., Huang, S.B. and Weller, D.D. (1996) Resistance of morpholino phosphorodiamidate oligomers to enzymatic degradation. *Antisense Nucleic Acid Drug Dev.*, **6**, 267–272.
20. Moulton, H.M. and Moulton, J.D. (2010) Morpholinos and their peptide conjugates: therapeutic promise and challenge for Duchenne muscular dystrophy. *Biochim. Biophys. Acta*, **1798**, 2296–2303.
21. Popplewell, L.J., Malerba, A. and Dickson, G. (2012) Optimizing antisense oligonucleotides using phosphorodiamidate morpholino oligomers. *Methods Mol. Biol.*, **867**, 143–167.
22. Iversen, P.L., Aird, K.M., Wu, R., Morse, M.M. and Devi, G.R. (2009) Cellular uptake of neutral phosphorodiamidate morpholino oligomers. *Curr. Pharm. Biotechnol.*, **10**, 579–588.
23. Mokri, B. and Engel, A.G. (1975) Duchenne dystrophy: electron microscopic findings pointing to a basic or early abnormality in the plasma membrane of the muscle fiber. *Neurology*, **25**, 1111–1120.
24. Yokota, T., Takeda, S., Lu, Q.-L., Partridge, T.A., Nakamura, A. and Hoffman, E.P. (2009) A renaissance for antisense oligonucleotide drugs in neurology: exon skipping breaks new ground. *Arch. Neurol.*, **66**, 32–38.
25. Hoffman, E.P., Bronson, A., Levin, A.A., Takeda, S., Yokota, T., Baudy, A.R. and Connor, E.M. (2011) Restoring dystrophin expression in Duchenne muscular dystrophy muscle progress in exon skipping and stop codon read through. *Am. J. Pathol.*, **179**, 12–22.
26. Florence, J.M., Fox, P.T., Planer, G.J. and Brooke, M.H. (1985) Activity, creatine kinase, and myoglobin in Duchenne muscular dystrophy: a clue to etiology? *Neurology*, **35**, 758–761.
27. Ozawa, E. (2010) Our trails and trials in the subsarcolemmal cytoskeleton network and muscular dystrophy researches in the dystrophin era. *Proc. Jpn. Acad. Ser. B Phys. Biol. Sci.*, **86**, 798–821.
28. Heemskerk, H., De Winter, C., Van Kuik, P., Heuvelmans, N., Sabatelli, P., Rimessi, P., Braghetta, P., Van Ommen, G.-J.B., De Kimpe, S., Ferlini, A. *et al.* (2010) Preclinical PK and PD studies on 2′-O-methyl-phosphorothioate RNA antisense oligonucleotides in the mdx mouse model. *Mol. Ther.*, **18**, 1210–1217.
29. Matsuda, R., Nishikawa, A. and Tanaka, H. (1995) Visualization of dystrophic muscle fibers in mdx mouse by vital staining with Evans blue: evidence of apoptosis in dystrophin-deficient muscle. *J. Biochem.*, **118**, 959–964.
30. Straub, V., Rafael, J.A., Chamberlain, J.S. and Campbell, K.P. (1997) Animal models for muscular dystrophy show different patterns of sarcolemmal disruption. *J. Cell Biol.*, **139**, 375–385.
31. Wood, M.J.A., Gait, M.J. and Yin, H. (2010) RNA-targeted splice-correction therapy for neuromuscular disease. *Brain*, **133**, 957–972.
32. Nakamura, A. and Takeda, S. (2011) Exon-skipping therapy for Duchenne muscular dystrophy. *Lancet*, **378**, 546–547.
33. Yokota, T., Nakamura, A., Nagata, T., Saito, T., Kobayashi, M., Aoki, Y., Echigoya, Y., Partridge, T., Hoffman, E.P. and Takeda, S. (2012) Extensive and prolonged restoration of dystrophin expression with vivo-morpholino-mediated multiple exon skipping in dystrophic dogs. *Nucleic Acid Ther.*, **22**, 306–315.
34. Ezzat, K., Helmfors, H., Tudoran, O., Juks, C., Lindberg, S., Padari, K., El-Andaloussi, S., Pooga, M. and Langel, U. (2012) Scavenger receptor-mediated uptake of cell-penetrating peptide nanocomplexes with oligonucleotides. *FASEB J.*, **26**, 1172–1180.
35. Moulton, H.M., Fletcher, S., Neuman, B.W., McClorey, G., Stein, D.A., Abes, S., Wilton, S.D., Buchmeier, M.J., Lebleu, B. and Iversen, P.L. (2007) Cell-penetrating peptide-morpholino conjugates alter pre-mRNA splicing of DMD (Duchenne muscular dystrophy) and inhibit murine coronavirus replication in vivo. *Biochem. Soc. Trans.*, **35**, 826–828.
36. Yin, H., Moulton, H.M., Betts, C., Merritt, T., Seow, Y., Ashraf, S., Wang, Q., Boutilier, J. and Wood, M.J. (2010) Functional rescue of dystrophin-deficient mdx mice by a chimeric peptide-PMO. *Mol. Ther.*, **18**, 1822–1829.
37. Moulton, H.M., Nelson, M.H., Hatlevig, S.A., Reddy, M.T. and Iversen, P.L. (2004) Cellular uptake of antisense morpholino oligomers conjugated to arginine-rich peptides. *Bioconjug. Chem.*, **15**, 290–299.
38. Amantana, A., Moulton, H.M., Cate, M.L., Reddy, M.T., Whitehead, T., Hassinger, J.N., Youngblood, D.S. and Iversen, P.L. (2007) Pharmacokinetics, biodistribution, stability and toxicity of a cell-penetrating peptide-morpholino oligomer conjugate. *Bioconjug. Chem.*, **18**, 1325–1331.
39. Henry, S.P., Giclas, P.C., Leeds, J., Pangburn, M., Auletta, C., Levin, A.A. and Kornbrust, D.J. (1997) Activation of the alternative pathway of complement by a phosphorothioate oligonucleotide: potential mechanism of action. *J. Pharmacol. Exp. Ther.*, **281**, 810–816.
40. Sheehan, J.P. and Lan, H.C. (1998) Phosphorothioate oligonucleotides inhibit the intrinsic tenase complex. *Blood*, **92**, 1617–1625.
41. Hawke, T.J. and Garry, D.J. (2001) Myogenic satellite cells: physiology to molecular biology. *J. Appl. Physiol.*, **91**, 534–551.
42. Miyagoe-Suzuki, Y., Nakagawa, M. and Takeda, S. (2000) Merosin and congenital muscular dystrophy. *Microsc. Res. Tech.*, **48**, 181–191.
43. Gawlik, K.I. and Durbeej, M. (2011) Skeletal muscle laminin and MDC1A: pathogenesis and treatment strategies. *Skeletal Muscle*, **1**, 9.
44. Sunada, Y., Bernier, S.M., Utani, A., Yamada, Y. and Campbell, K.P. (1995) Identification of a novel mutant transcript of laminin alpha 2 chain gene responsible for muscular dystrophy and dysmyelination in dy2J mice. *Hum. Mol. Genet.*, **4**, 1055–1061.
45. Allamand, V. and Guicheney, P. (2002) Merosin-deficient congenital muscular dystrophy, autosomal recessive (MDC1A, MIM#156225, LAMA2 gene coding for alpha2 chain of laminin). *Eur. J. Hum. Genet.*, **10**, 91–94.
46. Cartegni, L., Wang, J., Zhu, Z., Zhang, MQ. and Krainer, AR. (2003) ESEfinder: A web resource to identify exonic splicing enhancers. *Nucleic Acids Res.*, **31**, 3568–3571.